Atmos. Chem. Phys. Discuss., 10, 12309–12339, 2010
www.atmos-chem-phys-discuss.net/10/12309/2010/
doi:10.5194/acpd-10-12309-2010

Atmospheric Chemistry and Physics Discussions

Heterogeneous reactions of carbonyl sulfide on mineral oxides: mechanism and kinetics study

Y. Liu, J. Ma, and H. He

State Key Laboratory of Environmental Chemistry and Ecotoxicology, Research Center for Eco-Environmental Sciences, Chinese Academy of Sciences, Beijing, 100085, China

Received: 20 April 2010 – Accepted: 6 May 2010 – Published: 10 May 2010

Correspondence to: H. He (honghe@rcees.ac.cn)

Published by Copernicus Publications on behalf of the European Geosciences Union.

Abstract

The heterogeneous reactions of carbonyl sulfide (OCS) on the typical mineral oxides in the mineral dust particles were investigated using a Knudsen cell flow reactor and an in situ diffuse reflectance UV-vis spectroscopy. The reaction pathway for OCS on mineral dust was identified based on the gaseous products and surface species. The hydrolysis of OCS, and succeeding oxidation of intermediate products, readily take place on α-Al_2O_3, MgO, and CaO. The reversible and irreversible adsorption of OCS on α-Fe_2O_3 and ZnO were observed, respectively. No uptake of OCS by SiO_2 and TiO_2 was observed. The uptake coefficient (γ_{BET}) of mineral dust was estimated to be from 3.84×10^{-7} to 2.86×10^{-8} based on the individual uptake coefficients and chemical composition of authentic mineral dust. The global flux of OCS due to heterogeneous reactions and adsorption on mineral dust was estimated at 0.13–0.29 Tg yr^{-1}, which is comparable to the annual flux of OCS for its reaction with ·OH.

1 Introduction

Carbonyl sulfide (OCS) is the predominant sulfur containing compound in the atmosphere, with a rather uniform mixing ratio of about 500 pptv in the troposphere (Chin and Davis, 1995). About 0.64 Tg yr^{-1} of OCS in the troposphere is transported to the stratosphere, where it can be photodissociated as well as oxidized via reactions with O(^{3}P) atoms and OH radicals to form sulfate aerosols. Therefore, it has been considered to be a major source of the stratospheric sulfate aerosol (SSA) during volcanic quiescent periods (Andreae and Crutzen, 1997; Crutzen, 1976; Notholt, 2003; Turco et al., 1980). Because the SSA plays an important role in the Earth's radiation balance, global climate (Anderson, et al., 2003; Graf, 2004; Jones et al., 1994), and stratospheric ozone depletion (Andreae and Crutzen, 1997; Solomon et al., 1993), the investigation about the sources and sinks of OCS in the troposphere is very significant in atmospheric chemistry.

In the past decades, the heterogeneous reactions of trace gases in the atmosphere on atmospheric particles has become increasingly important (Ravishankara, 1997), because they not only account for the alteration of the particulate composition and its surface properties (Aubin and Abbatt, 2006; Jang et al., 2002) but also affect the sources and sinks of trace gases (Jacob, 2000). Several atmospheric modeling studies have shown that atmospheric particles often acting as a sink for certain species (Dentener et al., 1996; Usher et al., 2003b). A major contributor to the loading of atmospheric particles is mineral dust, which mainly originates from arid and semi-arid regions with global source strength of about 1000-3000 $Tg{\cdot}yr^{-1}$ (Dentener et al., 1996). The surface oxygen, hydroxyl group, absorbed water and defect sites on mineral oxides may provide reactive sites for the heterogeneous uptake of trace gases. Recently, using infrared spectroscopy, a few researchers have reported the heterogeneous reactions mechanism of OCS on atmospheric particles, and mineral oxides including Al_2O_3, SiO_2, Fe_2O_3, CaO, MgO, MnO_2 and the mixture of Fe_2O_3 and NaCl (Chen et al., 2007; He et al., 2005; Liu et al., 2006, 2007a, b, 2009a; Wu et al., 2004, 2005). In these studies, hydrogen thiocarbonate ($HSCO_2^-$) was found as a key intermediate (He et al., 2005; Liu et al., 2006, 2007a, b, 2009a). Gaseous carbon dioxide (CO_2) and surface sulfate (SO_4^{2-}) were found to be the gaseous and surface products (Chen et al., 2007; He et al., 2005; Liu et al., 2006, 2007a, b, 2009a), respectively. Surface sulfite and element sulfur were also observed as surface sulfur species (Wu et al., 2004, 2005). Additionally, gaseous hydrogen sulfide (H_2S) was detected as one of the hydrolysis products for the heterogeneous reaction of OCS on MgO and Al_2O_3 (Liu et al., 2007a, 2008a, b, 2009b). The previous works demonstrate that heterogeneous reactions on mineral dust may be a potential sink for OCS in the troposphere. However, besides on $Al_2O_3$and MgO, the reactions on all of the other oxides were mainly investigated using infrared spectroscopy with a high OCS concentration. Thus, the reaction pathway on these mineral oxides still needs to be further identified by other experimental methods. In particular, the difference in reaction pathway on these oxides is unclear. On the other hand, the significance of these reactions on the global chemical cycle of

OCS depends on its reaction rates or uptake coefficients. However, at present day, the uptake coefficients of OCS on the typical mineral oxides are very limited. Therefore, the kinetic study for the heterogeneous reactions of OCS on mineral dust is necessary.

In this study, besides α-Al_2O_3 and MgO as reported previously (Liu et al., 2008a, b, 2009b), we further investigated the heterogeneous reactions of OCS on the typical mineral oxide components in atmospheric particles, including SiO_2, CaO, α-Fe_2O_3, ZnO, and TiO_2, using a Knudsen cell reactor and a diffuse reflectance UV-vis spectroscopy. To facilitate comparison, the results of α-Al_2O_3 and MgO were also included. It revealed that the reactions could readily take place on some mineral oxides and some differences in reaction pathway exist on these oxides. On the basis of the uptake coefficients measured by Knudsen cell reactor, the environmental implications were discussed.

2 Experimental section

2.1 Materials

All of the chemicals were used with received. These included: Carbonyl sulfide (OCS, 1.98%, OCS/N_2, Scott Specialty Gases Inc.), N_2 and O_2 (99.999% purity, Beijing AP Beifen Gases Inc.), and C_2H_5OH (99.7%, Beijing Chemicals Factory).

According to the main composition of authentic mineral dust (He et al., 2005) and the upper continental crust (Usher et al., 2003a), SiO_2, α-Al_2O_3, CaO, MgO, α-Fe_2O_3, ZnO, and TiO_2 were chose as model dust samples. α-Al_2O_3 was prepared through calcining AlOOH (Shandong Alumina Corpartion) at 1473 K for 3 h. All of the other oxides are of analytic purity grade, including SiO_2 and TiO_2 (Beijing Yili Fine Chemicals Co. Ltd), α-Fe_2O_3 (Beijing Nanshang Chemicals Factory), CaO and ZnO (Shantou Nongxi Chemicals Factory Guangdong), and MgO (Tianjin Hangu Haizhong Chemicals Factory).

2.2 Characterization of sample

X-ray powder diffraction pattern was collected from 10 to 90°2θ on a D/max-RB automatic powder X-ray diffractometer using Cu Kα irradiation. Nitrogen Brunauer-Emmett-Teller (BET) physisorption measurement was performed with a Micromeritics ASAP 2000 analyzer.

2.3 Experimental methods

2.3.1 KCMS experiment

A Knudsen cell reactor coupled to a quadrupole mass spectrometer (KCMS, Hiden, HAL 3F PIC) was used to study the reaction pathway and to measure the uptake coefficients of OCS on the mineral oxides. The apparatus was described detailedly elsewhere (Liu et al, 2008a, b). Briefly, the mass spectrometer was housed in a vacuum chamber equipped with a 300 L s^{-1} turbomolecular pump (Pfeiffer) and an ion gauge (BOC Edward). The vacuum chamber between the quadrupole mass spectrometer (QMS) and the Knudsen cell reactor was pumped by a 60 L s^{-1} turbomolecular pump for differential pumping of the mass spectrometer and an ion gauge (both from BOC Edward).The Knudsen cell reactor consists of a stainless steel chamber with a gas inlet controlled by a leak valve, an escape aperture whose area could be adjusted with an adjustable iris and a sample holder attached to the top ceiling of a circulating fluid bath. The sample in the sample holder can be exposed or isolated to the reactants by a lid connected to a linear translator.

The oxide samples were dispersed evenly on the sample holder with alcohol and then dried at 393 K for 2 h. The pretreated samples and the reactor chamber were evacuated at 323 K for 6 h to reach a base pressure of approximately 5.0×10^{-7} Torr. After the system was cooled to 300 K, the sample cover was closed. 1.51% of OCS gas balanced with simulated air (21% O_2 and 79% N_2) was introduced into the reactor chamber through a leak valve. The relative humidity in the reactant gases was

measured to be 7% using a hygrometer (Center 314) with a relative error of ±1.5%. The pressure in reactor was measured using an absolute pressure transducer. Prior to the experiments, the reactor chamber was passivated with OCS in air for 150 min to a steady state of QMS signal established as the oxide samples were isolated from the gas by the sample cover. Uptake measurements on all samples were obtained with an average OCS partial pressure of $5.3\pm0.3\times10^{-6}$ Torr, which was equivalent to $1.7\pm0.2\times10^{11}$ molecules cm^{-3} or 7.0±0.3 ppbv. The uptake coefficients were calculated based on the KCMS signal. According to the pressure in the vacuum chamber and the pumping speeds of turbomolecular pumps, the mass signal intensity of OCS could be converted to flow rate of molecules into the reactor. Then adsorption capacity of OCS on mineral oxides could be calculated from the integrated area of a flow rate of molecules into the reactor versus time.

2.3.2 UV-vis experiment

The surface sulfur species on oxides after heterogeneous reaction with OCS were identified using a diffuse reflectance UV-vis Spectrophotometer (U-3310, Hitachi). 100 mg of mineral oxides in quartz tube were exposed to 1000 ppmv of OCS/air in the flow of 100 mL min^{-1} for 9 h at 300 K, and then the UV-vis spectra were collected promptly using the corresponding pure oxides as reference samples.

3 Results and discussion

3.1 Characterizations

XRD results indicate that these oxides used in experiment are quartz (SiO_2), corundum (α-Al_2O_3), lime (CaO), hematite (MgO), periclase (α-Fe_2O_3), spartalite (ZnO), and anatase (TiO_2), respectively. The detailed information was described elsewhere (Liu et al., 2008b). Because of the strong basicity and hygroscopicity, CaO sample contains a small amount of $Ca(OH)_2$.

The surface areas of these oxides as shown in Table 1 are almost in the same order and close to the value of the authentic atmospheric particles (He et al., 2005).

3.2 Uptake of OCS and desorption behavior of surface species on mineral oxides

3.2.1 α-Al_2O_3

In our previous works (Liu et al., 2005, 2006, and 2008a), we have reported the hydrolysis reaction and oxidation pathways of OCS on Al_2O_3. To facilitate comparison, the Knudsen cell results on α-Al_2O_3 and MgO were also described here briefly. Figure 1 shows a typical KCMS profile for the uptake of OCS on 50.2 mg of α-Al_2O_3 at 300 K. 1.51% of OCS was balanced with simulated air and the average OCS partial pressure in the Knudsen cell reactor was $5.3\pm0.3\times10^{-6}$ Torr. The relative humidity in the reactant gases was measured to be 7%. As shown in Fig. 1, the consumption of OCS and desorption of CO_2 and H_2S after reaction can be seen clearly. As discussed in our previous work (Liu et al., 2008a), the hysteresis of CO_2 to OCS for QMS signals during uptake experiment was ascribed to the influence by the adsorption of CO_2 and the compensation by the fragment peak of OCS (CS). In the uptake experiment, we did not observe the production of H_2S along with the formation of CO_2. It implies that the adsorption ability of H_2S is stronger than that of CO_2. The further oxidation of adsorbed H_2S to other sulfur species (He, et al., 2005; Liu et al., 2006, 2007a; Wu, et al., 2004, 2005) may also lead to the unobservable increase in QMS signals for H_2S. In Fig. 1d, no desorption of OCS was observed in the in situ desorption experiment. It means that adsorbed OCS could be easily transformed to other species, and the reversed process hardly took place. In our previous works (He, et al., 2005; Liu et al., 2006, 2007a), we have observed the surface species including bicarbonate (HCO_3^-) at 1645 and 1407 cm^{-1}, carbonate (CO_3^{2-}) at 1533 cm^{-1}. These result confirmed the hydrolysis and oxidation reactions of OCS taking place on α-Al_2O_3.

3.2.2 MgO and CaO

Figures 2 and 3 show the heterogeneous reactions of OCS on 100.0 mg of MgO and 100.4 mg of CaO at 300 K, respectively. As shown in Fig. 2, the uptake of OCS (m/e=60) was companied by the production of CO_2 (m/e=44) and H_2S (m/e=34) on MgO. In our previous works (Liu et al., 2007a, 2009a), we also observed the formation of gaseous CO_2 at 2341 and 2361 cm^{-1}, and surface HS at 2578 cm^{-1} using in situ DRIFTS studying the heterogeneous reaction of OCS on MgO at 303 K. Interestingly, in Fig. 2(A-C), the maximal yields of CO_2 and H_2S lagged behind the maximal consumption of OCS. This phenomenon was ascribed to the adsorption of CO_2 and H_2S on the basic site of MgO. Additionally, we have measured the decomposition rate of $HSCO_2^-$ to be $0.214\pm0.052\ s^{-1}$ and the adsorption rate constant of OCS to be $0.615\pm0.076\ s^{-1}$ on MgO at 300 K (Liu et al., 2008b). It suggests that the production of CO_2 and H_2S via $HSCO_2^-$ should be the rate determine step (RDS), thus, also leading to this hysteresis. The maximal yield of H_2S was also later than that of CO_2 because the acidity of H_2S is stronger than that of CO_2 and thus H_2S is more readily to be adsorbed on the basic site of MgO. These results also indicate heterogeneous hydrolysis of OCS taking place on MgO.

Although CaO is also a type of *FCC* crystalline of alkaline earth oxide as same as MgO, the uptake profiles of OCS on CaO were quite different from that on MgO as shown in Fig. 3. They are also different from that on α-Al_2O_3. The uptake of OCS on CaO was accompanied by the production of CO_2, while no formation of H_2S was detected. In our previous work (Liu et al., 2007b), surface CO_3^{2-}, HCO_3^-, SO_4^{2-}, and SO_3^{2-} were observed while no surface HS was observed for the heterogeneous reaction of OCS on CaO using in situ DRIFTS. In addition, except for CO_2, no desorptions of OCS and H_2S were observed in the in situ desorption experiment as shown in Fig. 3(D-F). These results suggest that the reaction pathway of OCS on CaO might be different from that on MgO and α-Al_2O_3. However, it should be pointed out that if H_2S produced by heterogeneous reaction on the surface of oxides can be easily and quickly transformed

into other species, it is hard to detect the surface HS or gaseous H_2S in DRIFTS and KCMS experiments.

3.2.3 α-Fe_2O_3 and ZnO

Figures 4 and 5 show the heterogeneous uptake of OCS and desorption of surface species on 141.3 mg of α-Fe_2O_3 and 200.9 mg of ZnO at 300 K, respectively. As the sample cover was opened, the mass signal intensity of OCS (m/e=60) decreased dramatically on both of these two samples (Figs. 4a and 5a). Although the total surface areas of α-Fe_2O_3 and ZnO used in this experiment were lower than that of α-Al_2O_3, MgO, and CaO, the dropping amplitude for the relative intensity of OCS in Figs. 4a and 5a were much larger than that in Figs. 1–3. However, the signal intensity of OCS quickly recovered to its baseline within 10 min. It suggests that the active sites for effectively uptaking OCS onto α-Fe_2O_3 and ZnO are very abundant, while they have lower catalytic reactivity for OCS hydrolysis or oxidation. In Figs. 4 and 5, the increasing of signal intensity for CO_2 was very weak and the change of signal intensity for H_2S was also negligible. In the end of uptake experiment, desorption of OCS was very distinct (Fig. 4d), while desorption of CO_2 was very weak (Fig. 4e) and no desorption of H_2S (Fig. 4f) was observed. Additionally, in Fig. 5d–f, no desorptions of OCS, CO_2, and H_2S were observed. Therefore, these results suggest that OCS might be reversibly adsorbed on α-Fe_2O_3 and irreversibly adsorbed on ZnO.

In our previous work, we found that when α-Fe_2O_3 and ZnO were exposed to OCS at 303 K for a long time (120 min), the consumption of surface hydroxyl was prominent and accompanied by the very weak absorbance of $HSCO_2^-$, HCO_3^-, and SO_4^{2-} etc. (Liu et al., 2007b). Recently, Chen et al. (2007) also observed the consumption of OCS on α-Fe_2O_3 for 24 h, while the reaction rate constant was measured to be very low. It should be noted that in these previous works (Chen et al., 2007; Liu et al., 2007b), the uptake experiments were investigated using DRIFTS reactors with a long exposure time. Thus, they obtained the integrated signals for the reaction on α-Fe_2O_3, while the differential signals was gained within a 0.6 s time-scale in this work. Therefore, the

uptake experiments performed in Knudsen cell reactor represent more initial and fresh state for oxides. Because the reactions of OCS on α-Fe_2O_3 and ZnO were also found to be very slow even though in the DRIFTS reactors, according to uptake experiments performed in this work, we think that OCS should be mainly reversibly adsorbed on α-Fe_2O_3 and irreversibly adsorbed on ZnO, and the hydrolysis and oxidation reactions on them are negligible.

3.2.4 SiO_2 and TiO_2

The uptake profiles of OCS on SiO_2 and TiO_2 are shown in Fig. 6. When 350.5 mg of SiO_2 and 400.0 mg of TiO_2 were exposed to the feed gas, respectively, no uptakes of OCS were observed in Fig. 6a and d. The changes of CO_2 and H_2S were also negligible when the sample cover was opened. In our previous work, we had observed the consumption of OCS over SiO_2 and TiO_2 in closed system were faintly faster than that over the background of in situ DRIFTS reactor chamber (Liu et al., 2007b). As discussed above, the difference between KCMS experiments and in situ DRIFTS experiments is derived from the different experimental methods. KCMS is a differential reactor, when the change of the flow rate of OCS in the reactor is lower than 2×10^{14} molecules s^{-1} (3σ), the QMS can not detect any change of its signal intensity, while the in situ DRIFTS reactor chamber in the closed system belongs to an integrated reactor, and the consumption of OCS is the accumulation of infrared signal at several minutes or several hours level. Therefore, we can conclude that even though the heterogeneous reactions of OCS can take place on SiO_2 and TiO_2, they are very slow and have little contribution to the sink of OCS in the troposphere.

3.3 Identification of other surface species and reaction pathway

Using DRIFTS, we have identified the surface species including $HSCO_2^-$, HS, CO_3^{2-}, HCO_3^-, SO_3^{2-}, and SO_4^{2-} etc. for the hydrolysis and oxidation of OCS on most of these oxides (Liu et al., 2005, 2006, 2007a, b, 2009a). Wu et al. (2004, 2005) also observed

the formation of element sulfur by XPS. In order to identify other surface species during heterogeneous reactions and to further clarify the difference between the reaction pathway of OCS on CaO and that on MgO (as shown in Figs. 2 and 3), the surface sulfur containing species were investigated by diffuse reflectance UV-vis spectroscopy. After the CaO and MgO samples were exposed to 1000 ppmv of OCS/air in 100 mL/min at 300 K for 9h, the diffuse reflectance UV-vis spectra were collected immediately using the corresponding pure oxides as reference samples. The UV-vis spectra are shown in Fig. 7. The peak at 217 nm is assigned to surface HSO_3^-, and the peak at 226 nm is ascribed to surface S^{2-}(Davydov, 2003). The abroad bands around 260–280 nm, and 340 nm were also observed and are assigned to the absorbance bands of element sulfur (Davydov, 2003).

As can be seen in Fig. 7, surface HSO_3^- and S^{2-} are the common surface sulfur containing species for the heterogeneous reaction of OCS on both CaO and MgO. The formation of HSO_3^- is well supported by the DRISFTS results (He et al., 2005; Liu et al., 2006, 2007a, b, 2009a). In Fig. 7a, very strong broad bands attributing to element sulfur were observed on CaO, which means element sulfur should also be one of the surface products for the heterogeneous reaction of OCS on CaO. It should be noted that S^{2-} were also observed for the OCS treated CaO sample. Therefore, we postulate that element S might be the further oxidization product of S^{2-}, while S^{2-} is result from the decomposition of H_2S or surface HS. This assumption is accordance with no desorption of H_2S after heterogeneous reaction of OCS on CaO (Fig. 3f). Additionally, after heterogeneous reaction, the sample was purged further with pure O_2 for 9 h and the absorbance of elemental sulfur decreased greatly (not shown). It means the newly formed sulfur can be further oxidized to high state species. As for MgO, although element S can be also observed (Fig. 7b), its relative content was much lower that that on CaO. It implies a low decomposition rate of surface HS to S on MgO, thus the formation and desorption of H_2S was very prominent (Fig. 2c and f), and the surface HS was also observable in the in situ infrared spectra (Liu et al., 2007a). As for OCS treated α-$Fe_2O_3$and ZnO, the UV-vis signal (not shown) was very weak due to their low

reactivity.

According to perturbation theory and orbital mixing, the decomposition reactivity of H_2S on mineral oxides was found to be related to the band gap of oxides. The lower the band gap of the oxide, the higher the adsorption activity and decomposition reactivity of H_2S (Rodriguez et al., 1998). The band gap of CaO is 6.8 eV, while it is 7.7 eV for MgO (Baltache et al., 2004). It suggests that the decomposition reaction of H_2S on CaO should be more facile than that on MgO. Therefore, we can deduce that the absence of H_2S in the products for the heterogeneous reaction of OCS on CaO should be ascribed to the formation of CaS and element sulfur on the surface.

It should be noted that Fe and Zn are typical sulphophile elements. It has been found that H_2S undergoes complete decomposition on ZnO to form sulfide at 300 K (Lin et al., 1992; Rodriguez et al., 1998). On the other hand, the small band gap of ZnO (3.4 eV) (Rodriguez et al., 1998) also implied its strong decomposition ability for H_2S to surface sulfide or sulfur species. As for α-Fe_2O_3, the band gap is 2.2 eV, which means the stronger decomposition ability for H_2S to surface sulfide or sulfur species. However, in our previous work, we have found that reactivity of OCS on mineral oxides depends on the basicity of oxides, i.e., the stronger the basicity of oxide, the higher the reactivity of OCS on it (Liu et al., 2007b and 2009b). α-$Fe_2O_3$and ZnO are typical acidic oxides, which suggests very low heterogeneous reactivity. On the other hand, in Figs. 4 and 5, desorption of CO_2 on α-Fe_2O_3 and ZnO was negligible, which suggests the amount of H_2S produced in heterogeneous reaction should be negligible. In particular, the reversible adsorption of OCS on α-Fe_2O_3 was observed in Fig. 4. Therefore, even if hydrolysis of OCS could occur on α-Fe_2O_3 and ZnO, the surface sulfide or element sulfur species, which is easily formed on these oxides, should lead to the quick deactivation by blocking the active site for the heterogeneous reaction of OCS on α-Fe_2O_3 and ZnO. Thus, the oxides with stronger basicity and lower decomposition ability for H_2S to surface sulfide or element sulfur species should show higher catalytic activities for decomposition of adsorbed OCS than these oxides with the anti-properties. Thus the main heterogeneous process of OCS on α-Fe_2O_3

and ZnO may be the adsorption process and the catalytic reaction of OCS is less important.

Based on above results and the previous works (Chen et al., 2007; He et al., 2005; Liu et al., 2006, 2007a, b, 2009), the reaction pathway for OCS on mineral oxides was summarized in Scheme 1. Catalytic reactions are very obvious on MgO, CaO and α-Al_2O_3. The key intermediate of $HSCO_2^-$ can be directly oxidized to HSO_3^-, HCO_3^-, and SO_4^{2-}. It can also hydrolyze to form H_2S and CO_2. Gaseous H_2S can further decompose to sulfide compound (MS) and element sulfur on MgO and CaO. The surface sulfur species including sulfur, sulfide and sulfite can be finally oxidized to sulfate. Irreversible adsorption of OCS on ZnO and reversible adsorption of OCS on α-Fe_2O_3 can take place at 300 K. As for TiO_2 and SiO_2, no uptake of OCS was observed.

3.4 Reaction kinetics for the heterogeneous reaction of OCS on mineral oxides

Uptake coefficient, which demonstrates the activity of adsorption or reaction for heterogeneous process, was the most commonly used kinetic parameter in atmospheric chemistry and also in the model studies. It was defined by Eq. (1) (Underwood et al., 2000).

$$\gamma = \frac{-\frac{dn}{dt}}{\omega} \quad (1)$$

where $-\frac{dn}{dt}$ is the number of molecules lost from the gas phase per second due to the collision between gas molecules and solid surface (molecules s^{-1}); ω is the total number of gas-surface collisions per second. Based on the Knudsen cell experimental results, the observed uptake coefficients, γ_{obs}, of OCS on mineral oxides characterized by the loss of gaseous OCS can be calculated from Knudsen cell equation (Barone et al., 1997; Beichert and Finlayson-Pitts, 1996; Liu et al., 2008a, 2008b; Underwood et

al., 2000).

$$\gamma_{obs} = \frac{A_h}{A_s}\frac{(I_0 - I)}{I} \quad (2)$$

where, A_h is the effective area of the escape aperture (cm^2); A_s is the geometric area of the sample holder (cm^2); and I_0 and I are the mass spectral intensities of OCS with the sample holder closed and open, respectively. If the reactant gas can diffuse into the underlying layers for the multilayer powder sample, the effective collision area should be considered. Usually, the effective surface area was used. And then the true uptake coefficients, γ_t (BET), can be calculated from

$$\gamma_t = \text{slope} \cdot \left(\frac{A_s}{S_{BET}}\right) \quad (3)$$

where slope is the slope of plot of γ_{obs} and sample mass in linear region (mg^{-1}); S_{BET} is the specific surface area of particle sample ($cm^2\ mg^{-1}$) (Carlos-Cuellar et al., 2003).

The observed uptake coefficients calculated according to the geometric area of the sample holder at initial time (referred as γ_{obs} (Initial)) and at steady state (γ_{obs} (Steady state)) were plotted along with sample mass through the origin and are shown in Fig. 8a–c. As for α-Fe_2O_3 and ZnO, γ_{obs}(Initial) and adsorption capacities were given in Fig. 8d and 8e. The error bar was 15 % obtained from the repeated experiments. It can be seen from Fig. 8 that there was a strong linear dependence of γ_{obs} or adsorption capacity versus sample mass for all tested mineral oxides. It means the underlying layers of these oxide samples also contribute to the heterogeneous uptake and catalytic reaction under this experimental conditions. Therefore, γ_t (BET) can be calculated from the slope and specific area of oxides sample via Eq. (3). The γ_t (BET) of OCS on different oxides were presented in Table 1 and in the range of $10^{-7} - 10^{-8}$. The γ_t (Initial) were in the order: α-Fe_2O_3 >ZnO>CaO> α-Al_2O_3 >MgO>SiO_2, TiO_2, while the order of γ_t (Steady state) is MgO> α-Al_2O_3, CaO>ZnO, α-Fe_2O_3, SiO_2, TiO_2.

When the intensity of mass spectrometer for OCS was corrected with flow rate of molecules and the consumption of OCS by catalytic reaction was subtracted, the adsorption capacity of OCS on different oxides was calculated and shown in Table 1. As can be seen in Table 1, the values of initial uptake coefficients of OCS on α-Al_2O_3, MgO, CaO, α-Fe_2O_3, and ZnO were much greater than that of steady state uptake coefficients. In despite of large initial uptake coefficients for α-Fe_2O_3 and ZnO, their steady state uptake coefficients decreased to zero. As discussed above, the initial uptake was mainly due to the adsorption process, while the steady state uptake was related to the catalytic reaction. It means that only a part of adsorbed OCS can be transformed to $HSCO_2^-$, and then it decomposes into CO_2 and H_2S, while the decomposition of $HSCO_2^-$ is the rate determine step (Liu et al., 2008b). On the other hand, the surface species such as HCO_3^-, CO_3^{2-}, S^{2-}, S, SO_3^{2-}, and SO_4^{2-} also induced the decline of catalytic reactivity. Therefore, the initial uptake coefficients on all of these oxides are much higher than their steady state uptake coefficients. Among these surface species, sulfide species have a very prominent effect, especially on ZnO, and CaO. Although the initial uptake coefficients were very large on these oxides, the steady state uptake coefficients were very small because the sulfide or sulfur species could hardly desorb from the surface. In addition, as mentioned above, the heterogeneous reactivity of OCS on mineral dust is in relation to the surface basicity of oxides (Liu et al., 2007b and 2009b). The order of steady state uptake coefficients also supports the forenamed assumption. Except for CaO, which is related to the deactivation of surface sulfur species, the order of steady state uptake coefficients is almost the same as the basicity sequence of mineral oxides. Therefore, we can deduce that the alkali elements and alkaline-earth metals in the authentic atmospheric particles should promote the heterogeneous reaction of OCS in the troposphere.

According to the true uptake coefficients of single oxide and the mineral composition of authentic atmospheric particulate matter (He et al., 2005; Usher et al., 2003a), the

true uptake coefficient of authentic atmospheric mineral dust can be estimated from

$$\gamma_{\text{dust}} = \sum f_i \gamma_i \tag{4}$$

where γ_{dust} is the true uptake coefficient for mineral dust; f_i is the fraction of oxide in atmospheric mineral dust (He et al., 2005); γ_i is the true uptake coefficient of corresponding oxide (Usher, et al., 2002). The γ_{dust} was calculated to be from 3.84×10^{-7} (initial) to 2.86×10^{-8} (steady state). This value is comparable to the uptake coefficient of NO_2 on mineral dust (10^{-7}-10^{-8}) (Ullerstmal et al., 2003; Underwood, et al., 1999, 2000).

In our previous work (Liu et al., 2007b), we have found that the heterogeneous reaction of OCS on mineral oxides is a first-order reaction. Therefore, the reaction rate constant can be calculated from Eq. (5) (Ravishankara, 1997).

$$k_{\text{dust}} = \frac{\bar{v} \cdot \gamma_{\text{dust}} \cdot \text{SA}}{4} \tag{5}$$

Here, k_{dust} is the rate constant for the first-order reaction (s^{-1}); $\bar{v}$ is the average velocity of OCS molecules ($m\,s^{-1}$); $\gamma_{\text{dust}}$is the true uptake coefficient of mineral dust ($m^2\,m^{-3}$); SA is the globally-averaged dust surface area ($150\,\mu m^2\,cm^{-3}$) (de Reus, et al., 2000). The rate constants of OCS on mineral dust in the troposphere were estimated to be $4.69\times10^{-9}\,s^{-1}$ (initial) and $3.49\times10^{-10}\,s^{-1}$ (steady state).

4 Conclusions and atmospheric implications

In this work, the heterogeneous reactions of OCS on the typical mineral oxides were investigated by using Knudsen cell reactor and diffuse reflectance UV-vis spectroscopy. Catalytic hydrolysis and oxidation were observed on MgO, CaO and α-Al_2O_3. Reversible adsorption of OCS on α-Fe_2O_3 and irreversible adsorption on ZnO were observed. As for TiO_2 and SiO_2, no uptake of OCS was observed. For CaO, the de-

composition reactivity of hydrolysis product (H_2S) is stronger than that on MgO and α-Al_2O_3, which leads to the obvious deactivation of hydrolysis of OCS on CaO at steady state. The uptake coefficients (BET) of OCS on these oxides were measured to be in the range of 10^{-7}–10^{-8}, and are comparable with the uptake of NO_2 on mineral dust.

Because the initial uptake is mainly due to adsorption, the heterogeneous process of OCS on mineral dust could be divided into adsorption and catalytic reaction. In the real atmosphere, the uptake coefficients at steady state should be more representative than the initial uptake coefficients because once emitted into the atmosphere the fresh dust samples were often quickly aged by reactant gases. With the assumption of the total OCS mass of 4.63 Tg in the troposphere (Chin and Davis, 1995), and the first-order reaction rate constants of OCS on mineral dust (steady state), the global flux of OCS on mineral dust due to heterogeneous reactions was calculated to be 0.05 Tg yr^{-1}. Thus, this value, which is relating to the catalytic activity of dust, is very important to access the sinks of OCS due heterogeneous reaction.

Based on the adsorption capacity of each oxide and the mass fraction of oxide in atmospheric mineral dust, the equivalent adsorption capacity of mineral dust was calculated to be 8.00×10^{17} molecules g^{-1} based on Eq. (6).

$$Ac_{dust} = \sum_i f_i Ac_i \quad (6)$$

Where Ac is the adsorption capacity. The adsorption process might contribute the global sink of 0.08–0.24 Tg OCS $year^{-1}$ with the deposit of mineral dust (1000–3000 Tg $year^{-1}$). Therefore, considering both the adsorption and the catalytic reactions, the total sink of OCS due to mineral dust should be 0.13–0.29 Tg $year^{-1}$ via the adsorption and catalytic reaction of mineral dust. Compared with other sinks, this value might be equivalent to the annual flux for reaction of OCS with ·OH of 0.10 Tg yr^{-1} (Watts, 2000). Even though only the consumption by catalytic reaction was considered, the contribution of mineral dust to the sink of OCS should also be not ignored.

Of course, the real atmosphere is very complicated. For example, the relative humidity and coexisting gases such as CO_2, NO_x, SO_2, organic compounds, and alkali metal

in particles etc. may have a complex effect on the heterogeneous reaction of OCS on mineral dust. Our recent work (Liu et al., 2009b) demonstrates that adsorbed water on mineral oxides should restrict the heterogeneous reaction of OCS, while the basic membrane and the uncovered part by water still have catalytic activity. In addition, in this study, we did not consider the alkali metal (Na and K) in the oxides. However, our previous work found that strong basicity of oxide is in favor of the heterogeneous reaction of OCS. It means that the alkali metal should also promote this reaction. Therefore, our results in this study only present the case under clean and dry conditions. Whereas this study at least revealed that heterogeneous reactions of OCS on mineral dust in the troposphere should be considered for evaluating the atmospheric behavior of OCS.

Acknowledgement. This research was financially supported by the National Natural Science Foundation of China (40775081, 20937004, and 50921064). Yongchun Liu would also like to thank the President Scholarship of Chinese Academy of Sciences for the financial support.

References

Anderson, T. L., Charison, R. J., Schwartz, S. E., Knutti, R., Boucher, O., Rodhe, H., Heintzenberg, J.: Climate forcing by aerosols – a hazy picture, Science, 300, 1103–1104, 2003.

Andreae, M. O. and Crutzen, P. J.: Atmospheric aerosols: Biogeochemical sources and role in atmospheric chemistry, Science, 276, 1052–1058, 1997.

Aubin, D. G. and Abbatt, J. P.: Laboratory measurements of thermodynamics of adsorption of small aromatic gases to n–hexane soot surfaces, Environ. Sci. Technol., 40, 179–187, 2006.

Baltache, H., Khenata, R., Sahnoun, M., Driz, M., Abbar, B. and Bouhafs, B.: Full potential calculation of structural, electronic and elastic properties of alkaline earth oxides MgO, CaO and SrO, Phys. B, 344, 334–342, 2004.

Barone, S. B., Zondlo, M. A., and Tolbert, M. A.: A kinetic and product study of hydrolysis of $ClONO_2$ on type Ia polar stratospheric cloud materials at 185 K, J. Phys. Chem. A, 101, 8643–8652, 1997.

Beichert, P. and Finlayson-Pitts, B. J.: Knudsen cell studies of the uptake of gaseous HNO_3 and other oxides of nitrogen on solid NaCl: The role of surface-adsorbed water, J. Phys. Chem., 100, 15218–15228, 1996.

Carlos-Cuellar, S., Li, P., Christensen, A. P., Krueger, B. J., Burrichter, C., and Grassian, V. H.: Heterogeneous uptake kinetics of volatile organic compounds on oxide surface using a Knudsen cell reactor: Adsorption of acetic acid, formaldehyde, and methanol on α-Fe_2O_3, α-Al_2O_3, and SiO_2, J. Phys. Chem. A, 107, 4250–4261, 2003.

Chen, H. H., Kong, L. D., Chen, J. M., Zhang, R. Y., and Wang L.: Heterogeneous uptake of carbonyl sulfide on hematite and hematite-NaCl mixtures, Environ. Sci. Technol., 41, 6484–6490, 2007.

Chin, M. and Davis, D. D.: A reanalysis of carbonyl sulfide as a source of stratospheric background sulfur aerosol, J. Geophys. Res., 100, 8993–9005, 1995.

Crutzen, P. J.: The possible importance of CSO for the sulfate layer of the stratosphere, Geophys. Res. Lett., 3, 73–76, 1976.

Dentener, F. J., Carmichael, G. R., Zhang, Y., Lelieveld, J., and Crutzen, P. J.: Role of mineral aerosol as a reactive surface in the global troposphere, J. Geophys. Res., 101, 22869–22889, 1996.

de Reus, M., Dentener, F., Thomas, A., Borrmann, S., Ström, J., and Lelieveld, J.: Airborne observations of dust aerosol over the North Atlantic Ocean during ACE 2: Indications for heterogeneous ozone destruction, J. Geophys. Res., 105, 15263–15275, 2000.

Graf, H. F.: The complex interaction of aerosols and clouds, Science, 303, 1309–1311, 2004.

He, H., Liu, J. F., Mu, Y. J., Yu. Y. B., and Chen, M. X.: Heterogeneous oxidation of carbonyl sulfide on atmospheric particles and alumina, Environ. Sci. Technol., 39, 9637–9642, 2005.

Hoggan, P. E., Aboulayt, A., Pieplu, A., Nortier, P., and Lavalley, J. C.: Mechanism of COS hydrolysis on alumina, J. Catal., 149, 300–306, 1994.

Isoniemi, E., Pettersson, M., Khriachtchev, L., Lundell, J., and Räsänen, M.: Infrared spectroscopy of H_2S and SH in rare–gas matrixes, J. Phys. Chem. A, 103, 679–685, 1999.

Jacob, D. J.: Heterogeneous chemistry and tropospheric ozone, Atmos. Environ., 34, 2131–2159, 2000.

Jang, M., Czoschke, N. M., Lee, S., and Kamens, R. M.: Heterogeneous atmospheric aerosol production by acid–catalyzed particle reactions, Science, 298, 814–817, 2002.

Jones, A., Roberts, D. L., and Slingo, A.: A climate model study of indirect radiative forcing by anthoropogenic sulphate aerosols. Nature, 370, 450–453, 1994.

Lin, J. Y., May, J. A., Didziulis, S. V., and Solomon, E. I.: Variable-energy photoelectron spectroscopic studies of H_2S chemisorption on Cu_2O and ZnO single-crystal surfaces: HS– bonding to copper (I) and zinc (II) sites related to catalytic poisoning, J. Am. Chem. Soc., 114, 4718–

4727, 1992.

Liu, J. F., Yu, Y. B., Mu, Y. J., and He, H.: Mechanism of heterogeneous oxidation of carbonyl sulfide on Al_2O_3: An in situ diffuse reflectance infrared Fourier transform spectroscopy investigation, J. Phys. Chem. B, 110, 3225–3230, 2006.

Liu Y. C. and He, H.: Heterogeneous reactivity of carbonyl sulfide on α–Al_2O_3 and γ–Al_2O_3, Atmos. Environ., 42, 960–969, 2008a.

Liu, Y. C. and He, H.: Experimental and theoretical study of hydrogen thiocarbonate for heterogeneous reaction of carbonyl sulfide on magnesium oxide, J. Phys. Chem. A, 113, 3387–3394, 2009a.

Liu Y. C., He, H., and Ma, Q. X.: Temperature dependence of the heterogeneous reaction of carbonyl sulfide on magnesium oxide, J. Phys. Chem. A, 112, 2820–2826, 2008b.

Liu, Y. C., He, H., Xu, W. Q., and Yu, Y. B.: Mechanism of heterogeneous reaction of carbonyl sulfide on magnesium oxide, J. Phys. Chem. A, 111, 4333–4339, 2007a.

Liu, Y. C., Liu, J. F., He, H., Yu, Y. B., and Xue, L.: Heterogeneous oxidation of carbonyl sulfide on mineral oxides, Chinese Sci. Bull., 52, 2063–2071, 2007b.

Liu, Y., Ma, Q., and He, H.: Comparative study of the effect of water on the heterogeneous reactions of carbonyl sulfide on the surface of α-Al_2O_3 and MgO, Atmos. Chem. Phys., 9, 6273–6286, doi:10.5194/acp-9-6273-2009, 2009b.

Notholt, J., Kuang, Z., Rinsland, C. P., Toon, G. C., Rex, M., Jones, N., Albrecht, T., Deckelmann, H., Krieg, J., Weinzierl, C., Bingemer, H., Weller, R., and Schrems, O.: Enhanced upper tropical troposhperic COS: Impact on the stratospheric aerosol layer, Science, 300, 307–310, 2003.

Ravishankara, A. R.: Heterogeneous and multiphase chemistry in the troposphere, Science, 276, 1058–1065, 1997.

Rodriguez, J. A., Chaturvedi, S., Kuhn, M., and Hrbek, J.: Reaction of H_2S and S_2 with metal/oxide surfaces: Band–gap size and chemical reactivity, J. Phys. Chem. B, 102, 5511–5519, 1998.

Solomon, S., Sanders, R. W., Garcia, R. R., and Keys, J. G.: Increased chlorine dioxide over Antarctica caused by volcanic aerosols form Mount Pinatubo, Nature, 363, 245–248, 1993.

Turco, R. P., Whitten, R. C., Toon, O. B., Pollack, J. B., and Hamill, P.: OCS, stratospheric aerosols and climate, Nature, 283, 283–286, 1980.

Ullerstam, M., Johnson, M. S., Vogt, R., and Ljungstrm, E.: DRIFTS and Knudsen cell study of the heterogeneous reactivity of SO_2 and NO_2 on mineral dust, Atmos. Chem. Phys., 3,

2043–2051, doi:10.5194/acp-3-2043-2003, 2003.
Underwood, G. M., Li, P., Usher, C. R., and Grassian, V. H.: Determining accurate kinetic parameters of potentially important heterogeneous atmospheric reactions on solid particles surfaces with a Knudsen cell reactor. J. Phys. Chem. A, 104, 819–829, 2000.
Underwood, G. M., Miller, T. M., and Grassian, V. H.: Transmission FT–IR and Knudsen cell study of the heterogeneous reactivity of gaseous nitrogen dioxide on mineral oxide particles, J. Phys. Chem. A, 103, 6184–6190, 1999.
Usher, C. R., Al-Hosney, H., Carlos-Cuellar, S., and Grassian, V. H.: A laboratory study of the heterogeneous uptake and oxidation of sulfur dioxide on mineral dust particles, J. Geophys. Res., 107, 4713–4721, 2002.
Usher, C. R., Michel, A. E., and Grassian, V. H.: Reactions on mineral dust, Chem. Rev., 103, 4883–4939, 2003a.
Usher, C. R., Michel, A. E., Stec, D., and Grassian, V. H.: Laboratory studies of ozone uptake on processed mineral dust, Atmos. Environ., 37, 5337–5347, 2003b.
Watts, S. F.: The mass budgets of carbonyl sulfide, dimethyl sulfide, carbon disulfide and hydrogen sulfide, Atmos. Environ., 34, 761–779, 2000.
West, J., Wllianms, P., Young, N., Rhodes, C., and Hutchings, G. J.: Low temperature hydrolysis of carbonyl sulfide using γ-alumina catalysts, Catal. Lett., 74, 111–114, 2001.
Wu, H. B., Wang, X., and Cheng, J. M.: Photooxidation of carbonyl sulfide in the presence of the typical oxides in atmospheric aerosol, Sci. China. Ser. B Chem., 48, 31–37, 2005.
Wu, H. B., Wang, X., Cheng, J. M., Yu, H. K., Xue, H. X., Pan, X. X., and Hou, H. Q.: Mechanism of the heterogeneous reaction of carbonyl sulfide with typical components of atmospheric aerosol, Chinese Sci. Bull., 49, 1231–1235, 2004.

Table 1. Uptake coefficients and adsorption capacities of OCS on mineral oxides.

Oxide	S_{BET} ($m^2\,g^{-1}$)	Slope (mg^{-1})	Uptake coefficient (BET)		Adsorption capacity (molecules g^{-1})
α-Al_2O_3	12.00	1.13±0.13E-5 1.62±0.27E-6	Ini SS	4.95E-07 7.10E-08	2.93E18
MgO	14.59	1.34±0.17E-5 4.67±1.14E-6	Ini SS	4.83E-07 1.68E-07	4.62E18
CaO	6.08	7.32±0.19E-6 8.89±2.02E-7	Ini SS	6.33E-07 7.69E-08	1.48E17
α-Fe_2O_3	2.74	1.72±0.54E-5 0	Ini SS	3.30E-06 0	8.27E17
ZnO	2.75	4.08±0.98E-6 0	Ini SS	7.80E-07 0	3.49E17
SiO_2 TiO_2	4.80 12.74	0	Ini SS	0 0	0 0
Mineral dust*	–	–	Ini SS	3.84E-07 2.86E-08	8.00E17

Note: Ini – the initial uptake coefficient; SS – the steady state uptake coefficient at 30 min.
The value for mineral dust was calculated based on the uptake coefficients of individual oxide and its fraction in authentic mineral dust.

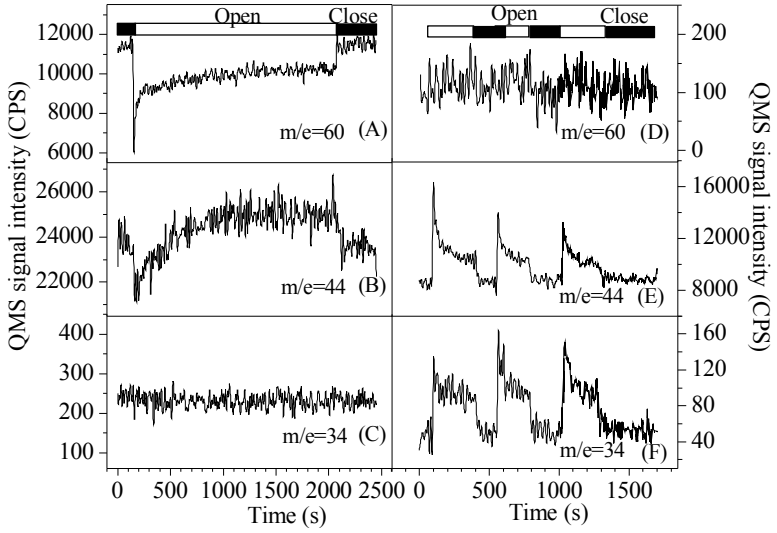

Fig. 1. The heterogeneous reaction of OCS on 50.2 mg of α-Al_2O_3 at 300 K (left side) and the in situ desorption of surface species in the end of uptake (right side).

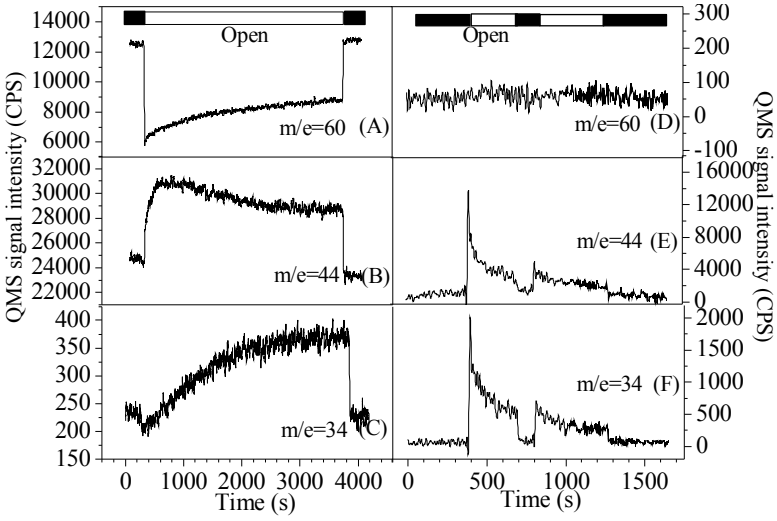

Fig. 2. The heterogeneous reaction of OCS on 100.0 mg of MgO at 300 K (left side) and the in situ desorption of surface species in the end of uptake (right side).

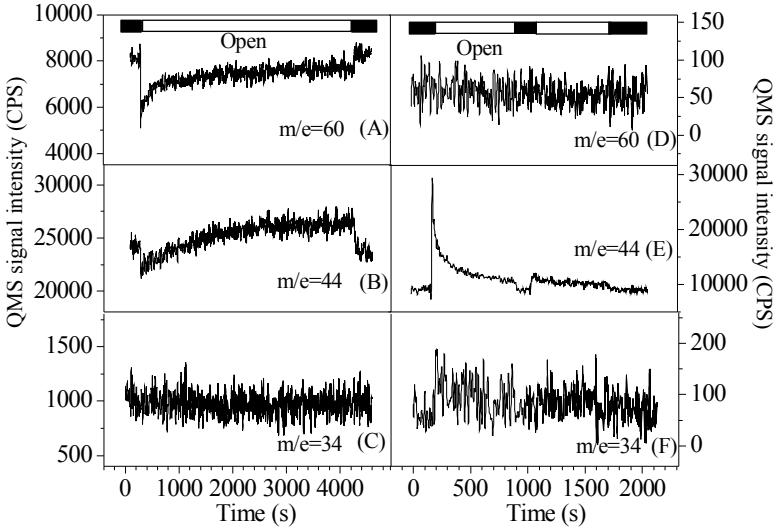

Fig. 3. The heterogeneous reaction of OCS on 100.4 mg of CaO at 300 K (left side) and the in situ desorption of surface species in the end of uptake (right side).

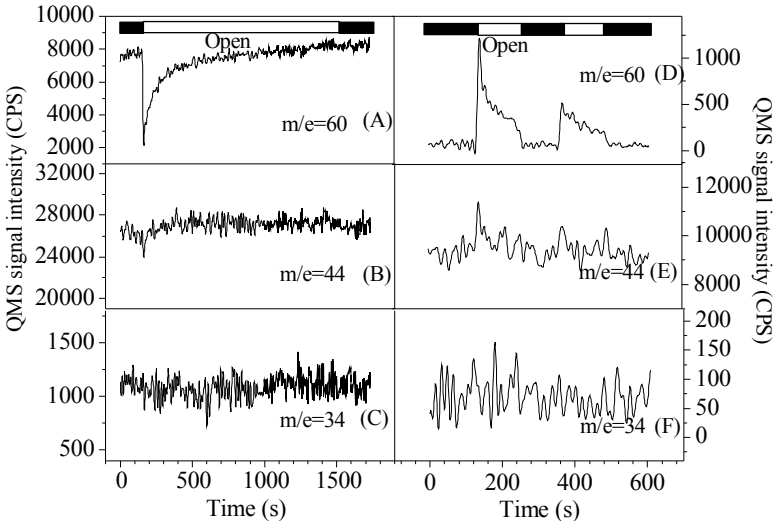

Fig. 4. The heterogeneous reaction of OCS on 141.3 mg of α-Fe_2O_3 at 300 K (left side) and the in situ desorption of surface species in the end of uptake (right side).

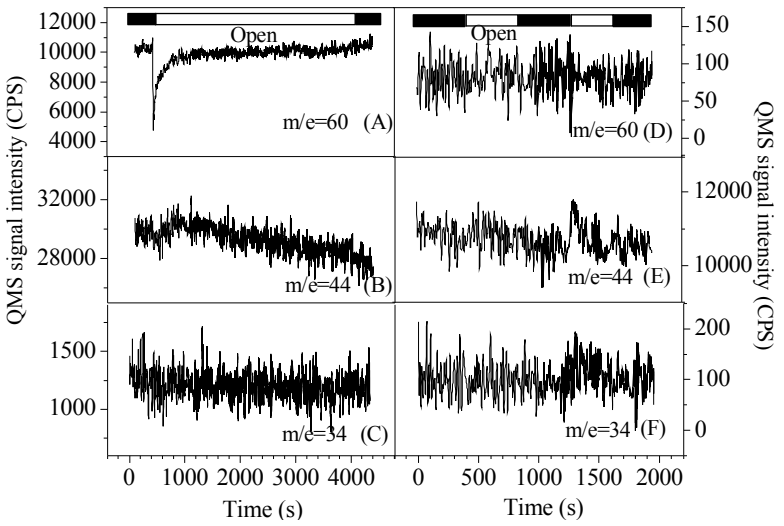

Fig. 5. The heterogeneous reaction of OCS on 200.9 mg of ZnO at 300 K (left side) and the in situ desorption of surface species in the end of uptake (right side).

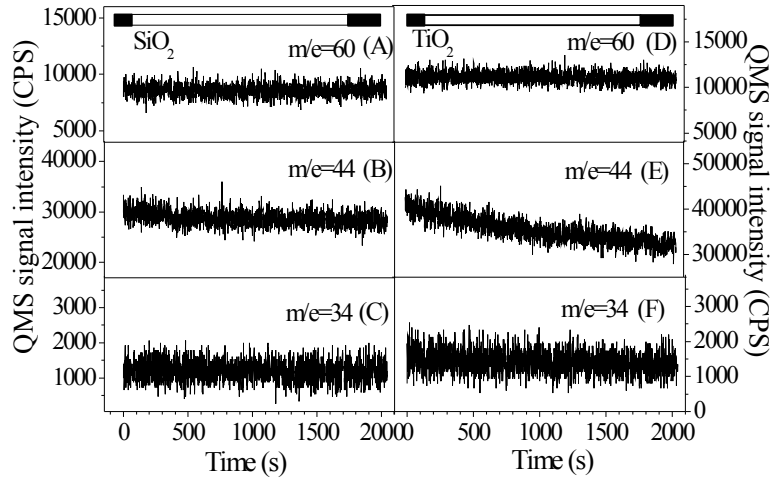

Fig. 6. The heterogeneous reactions of OCS on 350.5 mg SiO_2 and 400.0 mg TiO_2, respectively. The left side is the uptake curve of OCS by SiO_2, and the right side is the uptake curve of OCS by TiO_2.

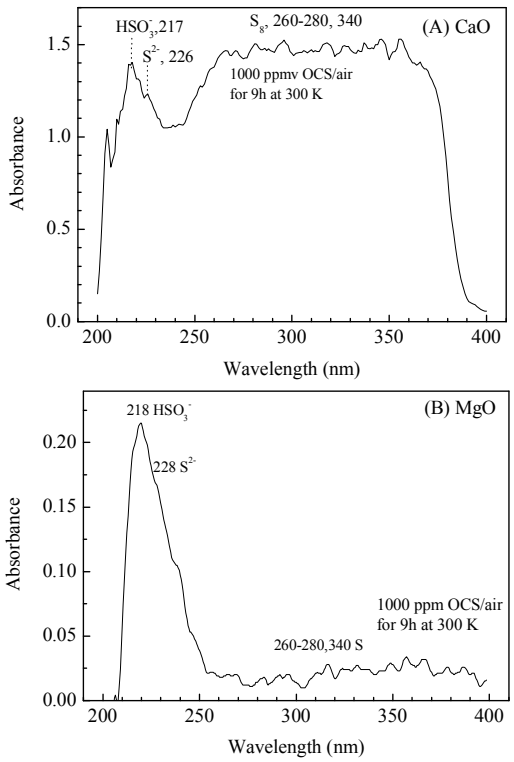

Fig. 7. Diffuse reflectance UV-vis spectra of **(A)** CaO, and **(B)** MgO after exposed to 1000 ppmv of OCS in air for 9 h.

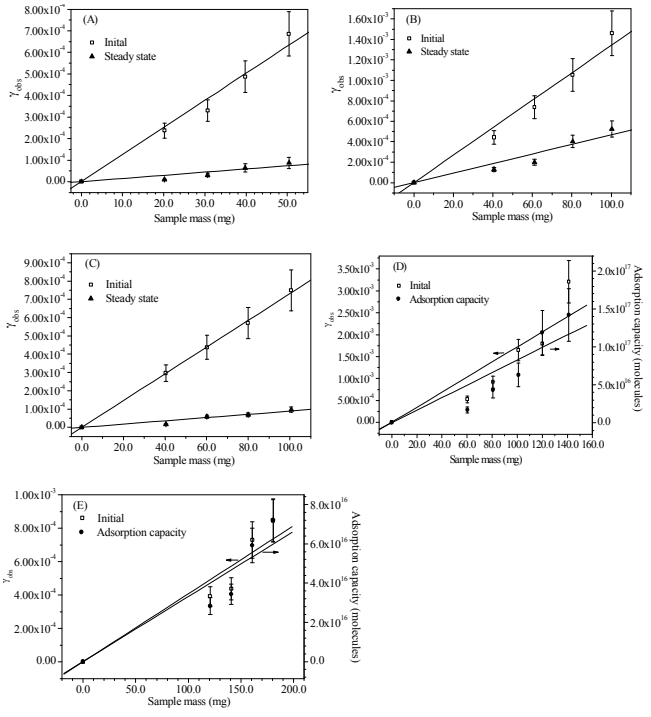

Fig. 8. The linear mass dependence between uptake coefficients or saturated adsorption capacity and sample mass for OCS on mineral oxides at 300 K. **(A)** α-Al_2O_3, **(B)** MgO, **(C)** CaO, **(D)** α-Fe_2O_3, **(E)** ZnO.

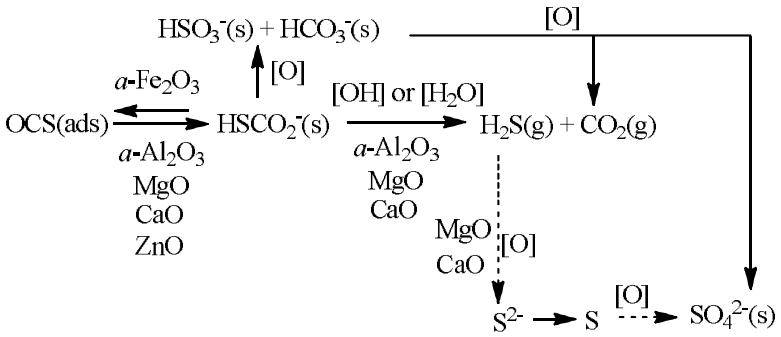

Scheme 1. Reaction pathway for OCS on different mineral oxides.